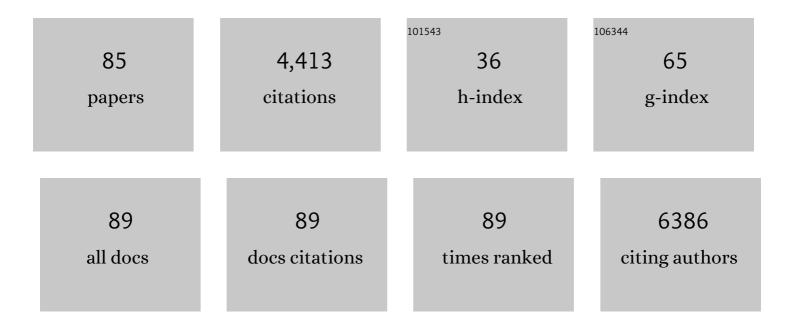
Tae-Wook Kim

List of Publications by Year in descending order

Source: https://exaly.com/author-pdf/8213972/publications.pdf Version: 2024-02-01



TAE-MOOK KIM

#	Article	IF	CITATIONS
1	Organic Resistive Memory Devices: Performance Enhancement, Integration, and Advanced Architectures. Advanced Functional Materials, 2011, 21, 2806-2829.	14.9	432
2	Evolution of nanomorphology and anisotropic conductivity in solvent-modified PEDOT:PSS films for polymeric anodes of polymer solar cells. Journal of Materials Chemistry, 2009, 19, 9045.	6.7	282
3	Quantum confinement effect in crystalline silicon quantum dots in silicon nitride grown using SiH4 and NH3. Applied Physics Letters, 2006, 88, 123102.	3.3	227
4	Threeâ€Dimensional Integration of Organic Resistive Memory Devices. Advanced Materials, 2010, 22, 5048-5052.	21.0	213
5	A New Approach for Molecular Electronic Junctions with a Multilayer Graphene Electrode. Advanced Materials, 2011, 23, 755-760.	21.0	171
6	Stable Switching Characteristics of Organic Nonvolatile Memory on a Bent Flexible Substrate. Advanced Materials, 2010, 22, 3071-3075.	21.0	164
7	Flexible and twistable non-volatile memory cell array with all-organic one diode–one resistor architecture. Nature Communications, 2013, 4, 2707.	12.8	156
8	Photoluminescence of silicon quantum dots in silicon nitride grown by NH3 and SiH4. Applied Physics Letters, 2005, 86, 091908.	3.3	120
9	Flexible Nanoporous WO _{3–<i>x</i>} Nonvolatile Memory Device. ACS Nano, 2016, 10, 7598-7603.	14.6	114
10	Highâ€Efficiency Photovoltaic Devices using Trapâ€Controlled Quantumâ€Dot Ink prepared via Phaseâ€Transfer Exchange. Advanced Materials, 2017, 29, 1605756.	21.0	114
11	Ultrathin Conformable Organic Artificial Synapse for Wearable Intelligent Device Applications. ACS Applied Materials & Interfaces, 2019, 11, 1071-1080.	8.0	106
12	One-dimensional organic artificial multi-synapses enabling electronic textile neural network for wearable neuromorphic applications. Science Advances, 2020, 6, .	10.3	102
13	One Transistor–One Resistor Devices for Polymer Nonâ€Volatile Memory Applications. Advanced Materials, 2009, 21, 2497-2500.	21.0	100
14	Graphene oxide nanosheets based organic field effect transistor for nonvolatile memory applications. Applied Physics Letters, 2010, 97, .	3.3	90
15	Synaptic Plasticity and Metaplasticity of Biological Synapse Realized in a KNbO ₃ Memristor for Application to Artificial Synapse. ACS Applied Materials & Interfaces, 2018, 10, 25673-25682.	8.0	85
16	Hierarchical Porous Film with Layer-by-Layer Assembly of 2D Copper Nanosheets for Ultimate Electromagnetic Interference Shielding. ACS Nano, 2021, 15, 829-839.	14.6	85
17	Rareâ€Earthâ€Elementâ€Ytterbiumâ€Substituted Leadâ€Free Inorganic Perovskite Nanocrystals for Optoelectronic Applications. Advanced Materials, 2019, 31, e1901716.	21.0	81
18	High Efficiency Low-Temperature Processed Perovskite Solar Cells Integrated with Alkali Metal Doped ZnO Electron Transport Layers. ACS Energy Letters, 2018, 3, 1241-1246.	17.4	77

#	Article	IF	CITATIONS
19	Shallow and Deep Trap State Passivation for Low-Temperature Processed Perovskite Solar Cells. ACS Energy Letters, 2020, 5, 1396-1403.	17.4	75
20	Facile and Purification-Free Synthesis of Nitrogenated Amphiphilic Graphitic Carbon Dots. Chemistry of Materials, 2016, 28, 1481-1488.	6.7	74
21	Highly efficient air-stable colloidal quantum dot solar cells by improved surface trap passivation. Nano Energy, 2017, 39, 86-94.	16.0	72
22	Degradation mechanism of planar-perovskite solar cells: correlating evolution of iodine distribution and photocurrent hysteresis. Journal of Materials Chemistry A, 2017, 5, 4527-4534.	10.3	69
23	Allâ€Organic Photopatterned One Diodeâ€One Resistor Cell Array for Advanced Organic Nonvolatile Memory Applications. Advanced Materials, 2012, 24, 828-833.	21.0	68
24	Influence of metal-molecule contacts on decay coefficients and specific contact resistances in molecular junctions. Physical Review B, 2007, 76, .	3.2	67
25	Reversible switching characteristics of polyfluorene-derivative single layer film for nonvolatile memory devices. Applied Physics Letters, 2008, 92, .	3.3	66
26	n-Doping of thermally polymerizable fullerenes as an electron transporting layer for inverted polymer solar cells. Journal of Materials Chemistry, 2011, 21, 6956.	6.7	60
27	Transient reverse current phenomenon in a p-n heterojunction comprised of poly(3,4-ethylene-dioxythiophene):poly(styrene-sulfonate) and ZnO nanowall. Applied Physics Letters, 2008, 93, .	3.3	55
28	Effects of Metalâ^'Molecule Contact and Molecular Structure on Molecular Electronic Conduction in Nonresonant Tunneling Regime: Alkyl versus Conjugated Molecules. Journal of Physical Chemistry C, 2008, 112, 13010-13016.	3.1	55
29	Ultrastrong Graphene–Copper Core–Shell Wires for High-Performance Electrical Cables. ACS Nano, 2018, 12, 2803-2808.	14.6	52
30	Electrical transport characteristics through molecular layers. Journal of Materials Chemistry, 2011, 21, 18117.	6.7	48
31	Resistive switching characteristics of polymer non-volatile memory devices in a scalable via-hole structure. Nanotechnology, 2009, 20, 025201.	2.6	47
32	2D Single rystalline Copper Nanoplates as a Conductive Filler for Electronic Ink Applications. Small, 2018, 14, 1703312.	10.0	47
33	Direct Synthesis of a Selfâ€Assembled WSe ₂ /MoS ₂ Heterostructure Array and its Optoelectrical Properties. Advanced Materials, 2019, 31, e1904194.	21.0	47
34	Layer-Selective Synthesis of MoS ₂ and WS ₂ Structures under Ambient Conditions for Customized Electronics. ACS Nano, 2020, 14, 8485-8494.	14.6	41
35	Three-Dimensional Porous Copper-Graphene Heterostructures with Durability and High Heat Dissipation Performance. Scientific Reports, 2015, 5, 12710.	3.3	40
36	Diphenylâ€2â€pyridylamineâ€&ubstituted Porphyrins as Holeâ€Transporting Materials for Perovskite Solar Cells. ChemSusChem, 2017, 10, 3780-3787.	6.8	40

#	Article	IF	CITATIONS
37	Nanoscale Resistive Switching of a Copper–Carbon-Mixed Layer for Nonvolatile Memory Applications. IEEE Electron Device Letters, 2009, 30, 302-304.	3.9	34
38	Triboelectric effect of surface morphology controlled laser induced graphene. Journal of Materials Chemistry A, 2020, 8, 19822-19832.	10.3	34
39	Low-Voltage Organic Transistor Memory Fiber with a Nanograined Organic Ferroelectric Film. ACS Applied Materials & Interfaces, 2019, 11, 22575-22582.	8.0	33
40	Channel-length and gate-bias dependence of contact resistance and mobility for In2O3 nanowire field effect transistors. Journal of Applied Physics, 2007, 102, 084508.	2.5	28
41	Effects of channel-length scaling on In2O3 nanowire field effect transistors studied by conducting atomic force microscopy. Applied Physics Letters, 2007, 90, 173106.	3.3	27
42	Integration of multiple electronic components on a microfibre towards an emerging electronic textile platform. Nature Communications, 2022, 13, .	12.8	27
43	Structure-controllable growth of nitrogenated graphene quantum dots via solvent catalysis for selective C-N bond activation. Nature Communications, 2021, 12, 5879.	12.8	25
44	Metal nanofibrils embedded in long free-standing carbon nanotube fibers with a high critical current density. NPG Asia Materials, 2018, 10, 146-155.	7.9	23
45	Characterization of PI:PCBM organic nonvolatile resistive memory devices under thermal stress. Organic Electronics, 2016, 33, 48-54.	2.6	22
46	Hybrid dielectrics composed of Al2O3 and phosphonic acid self-assembled monolayers for performance improvement in low voltage organic field effect transistors. Nano Convergence, 2018, 5, 20.	12.1	22
47	A direct metal transfer method for cross-bar type polymer non-volatile memory applications. Nanotechnology, 2008, 19, 405201.	2.6	21
48	Controllable Switching Filaments Prepared via Tunable and Well-Defined Single Truncated Conical Nanopore Structures for Fast and Scalable SiO _{<i>x</i>} Memory. Nano Letters, 2017, 17, 7462-7470.	9.1	21
49	Enhancement of Adsorption Performance for Organic Molecules by Combined Effect of Intermolecular Interaction and Morphology in Porous rGO-Incorporated Hydrogels. ACS Applied Materials & Interfaces, 2018, 10, 17335-17344.	8.0	21
50	Recent Advances in Fiber-Shaped Electronic Devices for Wearable Applications. Applied Sciences (Switzerland), 2021, 11, 6131.	2.5	21
51	Tunable rectification in a molecular heterojunction with two-dimensional semiconductors. Nature Communications, 2020, 11, 1412.	12.8	19
52	Direct-patterned copper/poly(ethylene oxide) composite electrodes for organic thin-film transistors through cone-jet mode by electrohydrodynamic jet printing. Journal of Industrial and Engineering Chemistry, 2020, 85, 269-275.	5.8	19
53	Resistive switching characteristics of ZnO–graphene quantum dots and their use as an active component of an organic memory cell with one diode-one resistor architecture. Organic Electronics, 2015, 18, 77-83.	2.6	18
54	Structurally Engineered Nanoporous Ta ₂ O _{5–<i>x</i>} Selector-Less Memristor for High Uniformity and Low Power Consumption. ACS Applied Materials & Interfaces, 2017, 9, 34015-34023.	8.0	18

#	Article	IF	CITATIONS
55	Highly Stable and Ultrafast Hydrogen Gas Sensor Based on 15 nm Nanogaps Switching in a Palladium–Gold Nanoribbons Array. Advanced Materials Interfaces, 2019, 6, 1801442.	3.7	18
56	Porous copper–graphene heterostructures for cooling of electronic devices. Nanoscale, 2017, 9, 7565-7569.	5.6	17
57	Reliable Organic Nonvolatile Memory Device Using a Polyfluorene-Derivative Single-Layer Film. IEEE Electron Device Letters, 2008, 29, 852-855.	3.9	16
58	Unsymmetrical Small Molecules for Broad-Band Photoresponse and Efficient Charge Transport in Organic Phototransistors. ACS Applied Materials & Interfaces, 2020, 12, 25066-25074.	8.0	16
59	Performance enhancement of graphene assisted CNT/Cu composites for lightweight electrical cables. Carbon, 2021, 179, 53-59.	10.3	15
60	One step synthesis of Au nanoparticle-cyclized polyacrylonitrile composite films and their use in organic nano-floating gate memory applications. Journal of Materials Chemistry C, 2016, 4, 1511-1516.	5.5	14
61	Hierarchical Hybrid Nanostructures Constructed by Fullerene and Molecular Tweezer. ACS Nano, 2019, 13, 6101-6112.	14.6	14
62	Molecular engineering of a porphyrin-based hierarchical superstructure: planarity control of a discotic metallomesogen for high thermal conductivity. Materials Horizons, 2020, 7, 2635-2642.	12.2	13
63	The Effect of Nanoscale Nonuniformity of Oxygen Vacancy on Electrical and Reliability Characteristics of \$hbox{HfO}_{2}\$ MOSFET Devices. IEEE Electron Device Letters, 2008, 29, 54-56.	3.9	12
64	Structure and Electrocatalysis of Sputtered RuPt Thin-Film Electrodes. Journal of Physical Chemistry B, 2005, 109, 12845-12849.	2.6	11
65	An All-Organic Composite System for Resistive Change Memory via the Self-Assembly of Plastic-Crystalline Molecules. ACS Applied Materials & Interfaces, 2017, 9, 2730-2738.	8.0	10
66	Fabrication of spray-printed organic non-volatile memory devices for low cost electronic applications. Materials Science and Engineering B: Solid-State Materials for Advanced Technology, 2015, 191, 51-56.	3.5	9
67	ZnO films using a precursor solution irradiated with an electron beam as the cathode interfacial layer in inverted polymer solar cells. RSC Advances, 2017, 7, 26689-26696.	3.6	9
68	Light-sensitive charge storage medium with spironaphthooxazine molecule-polymer blends for dual-functional organic phototransistor memory. Organic Electronics, 2020, 78, 105554.	2.6	8
69	Two-in-One Device with Versatile Compatible Electrical Switching or Data Storage Functions Controlled by the Ferroelectricity of P(VDF-TrFE) via Photocrosslinking. ACS Applied Materials & Interfaces, 2019, 11, 25358-25368.	8.0	7
70	Sandwich-Doping for a Large Schottky Barrier and Long-Term Stability in Graphene/Silicon Schottky Junction Solar Cells. ACS Omega, 2021, 6, 3973-3979.	3.5	7
71	High density silicon nanocrystal embedded in sin prepared by low energy (>500eV) SiH/sub 4/ plasma immersion ion implantation for non-volatile memory applications. , 0, , .		6
72	Allâ€Solidâ€State Organic Schmitt Trigger Implemented by Twin Twoâ€inâ€One Ferroelectric Memory Transistors. Advanced Electronic Materials, 2020, 6, 1901263.	5.1	5

#	Article	IF	CITATIONS
73	Interplay Among Thermoelectric Properties, Atmospheric Stability, and Electronic Structures in Solutionâ€Deposited Thin Films of P(Na _X [Niett]). Advanced Electronic Materials, 2020, 6, 1901172.	5.1	5
74	Tailoring the internal structure of porous copper film via size-controlled copper nanosheets for electromagnetic interference shielding. Materials Science and Engineering B: Solid-State Materials for Advanced Technology, 2022, 278, 115611.	3.5	5
75	In-Depth Study on the Effect of Active-Area Scale-Down of Solution-Processed \$hbox{TiO}_{x}\$. IEEE Electron Device Letters, 2012, 33, 869-871.	3.9	4
76	Meyer-Rod Coated 2D Single-Crystalline Copper Nanoplate Film with Intensive Pulsed Light for Flexible Electrode. Coatings, 2020, 10, 88.	2.6	3
77	All-Organic Photopatterned One Diode-One Resistor Cell Array for Advanced Organic Nonvolatile Memory Applications (Adv. Mater. 6/2012). Advanced Materials, 2012, 24, 827-827.	21.0	2
78	Large area thermal light emission from autonomously formed suspended graphene arrays. Carbon, 2018, 136, 217-223.	10.3	1
79	Comparisons of charge transport through alkane- monothiols and dithiols. , 2006, , .		0
80	Electronic transport in indium oxide nanowire field effect transistors. , 2006, , .		0
81	Length-dependent electronic transport through alkane-dithiol self-assembled monolayer junctions. , 2006, , .		Ο
82	Resistive switching characteristics of solution-processible TiO <inf>x</inf> using nano-scale via-hole structures. , 2009, , .		0
83	Heterostructure Arrays: Direct Synthesis of a Selfâ€Assembled WSe ₂ /MoS ₂ Heterostructure Array and its Optoelectrical Properties (Adv. Mater. 43/2019). Advanced Materials, 2019, 31, 1970309.	21.0	Ο
84	STATISTICAL ANALYSIS OF ELECTRONIC TRANSPORT PROPERTIES OF ALKANETHIOL MOLECULAR JUNCTIONS. , 2010, , 121-150.		0
85	Charge transport of alkanethiol self-assembled monolayers in micro-via hole devices. Journal of Nanoscience and Nanotechnology, 2006, 6, 3487-90.	0.9	0